Article

Calculations of the Effects of Substituents on Bond Localization in Annelated Cyclopentadienyl Radicals

Xin Zhou, David A. Hrovat, and Weston Thatcher Borden

J. Am. Chem. Soc., **2007**, 129 (35), 10785-10794• DOI: 10.1021/ja072314t • Publication Date (Web): 10 August 2007

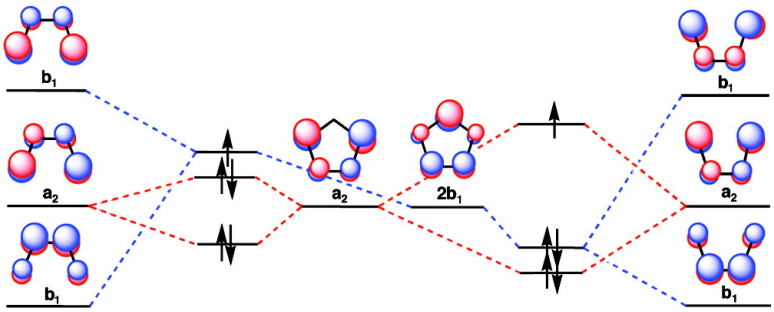

More About This Article

Additional resources and features associated with this article are available within the HTML version:

- Supporting Information
- Links to the 2 articles that cite this article, as of the time of this article download
- Access to high resolution figures
- Links to articles and content related to this article
- Copyright permission to reproduce figures and/or text from this article

View the Full Text HTML

J|A|C|S
ARTICLES
Published on Web 08/10/2007

Calculations of the Effects of Substituents on Bond Localization in Annelated Cyclopentadienyl Radicals

Xin Zhou, David A. Hrovat, and Weston Thatcher Borden*

Contribution from the Department of Chemistry, University of North Texas, P.O. Box 305070, Denton, Texas 76203-5070

Received April 2, 2007; E-mail: borden@unt.edu

Abstract: UB3LYP/6-31G(d) calculations have been performed in order to predict the ground states, $^2A_2$ or $^2B_1$, of cyclopentadienyl radicals that are mono- and bis-annelated with a wide variety of substituents. Unlike the case in the annelated cyclooctatetraenes, studied by Baldridge and Siegel, our calculations find that the sizes of the coefficients of the degenerate MOs at the annelated carbons are more important than the symmetries of the substituent's frontier orbitals in determining the mode of bond localization in the annelated cyclopentadienyl radicals.

Baldridge, Siegel, and co-workers first predicted computationally[1] and then confirmed experimentally[2] that annelation of benzene with three 1,3-bridged cyclobutane rings results in exocyclic localization of the benzene π bonds, as in the case of **1a**, rather than endocyclic localization, as in the case of **1b**. Explanations in terms of ring strain have been considered.[3] However, a preference for the stabilizing orbital interactions between the 1,3-bridged cyclobutane rings and butadiene bridges in **1a** over the destabilizing orbital interactions between the cyclobutane rings and the ethylene bridges in **1b**[4] provides a more attractive rationalization.[2b,3c,5,6]

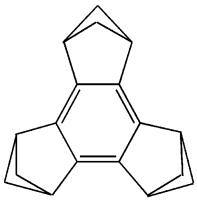

1a

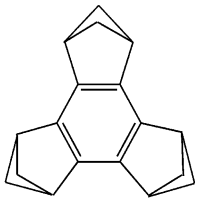

1b

Similarly, Baldridge and Siegel predicted computationally[5] and Komatsu subsequently confirmed experimentally[7] that annelation of cyclooctatetraene (COT) with four 1,3-bridged cyclobutane rings results in exocyclic localization of the double bonds, as in **2a**, rather than endocyclic localization, as in **2b**.

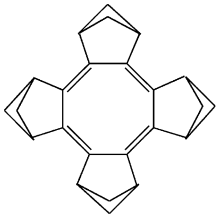

2a

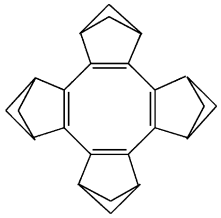

2b

However, exocyclic localization of the double bonds in annelated derivatives of COT is not always favored. For example, tetrakis(tetrafluoroethano)COT is known from X-ray crystallography to favor the endocyclic localization of the double bonds in **3b** over the exocyclic localization in **3a**.[8] Indeed, Baldridge and Siegel have carried out calculations that predict the mode of double bond localization in **3b** to be more favorable than that in **3a** by 17.2 kcal/mol.[5]

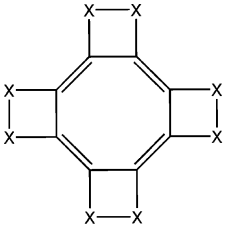

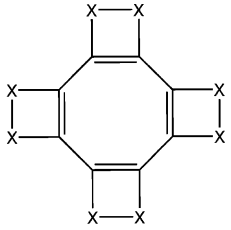

3a, X = CF_2
4a, X = C=O
5a, X = BH
6a, X = NH
7a, X-X = HC=CH

3b, X = CF_2
4b, X = C=O
5b, X = BH
6b, X = NH
7b, X-X = HC=CH

The difference between **2** and **3** in the preferred mode of double bond localization in the COT ring is easily explicable on the basis of orbital interactions.[6] Of the two possible π-like combinations of the low-lying, C−F antibonding orbitals of a

(1) Baldridge, K. K.; Siegel, J. S. *J. Am. Chem. Soc.* **1992**, *114*, 9583.
(2) (a) Frank, N. L.; Baldridge, K. K.; Siegel, J. S. *J. Am. Chem. Soc.* **1995**, *117*, 2102. (b) Bond localization, endocyclic to two, annelating, 1,3-bridged cyclobutane rings, has also been found experimentally to be disfavored in naphthalene; Uto, T.; Nishinaga, T.; Matsuura, A.; Inoue, R.; Komatsu, K. *J. Am. Chem. Soc.* **2005**, *127*, 10162.
(3) (a) Burgi, J. B.; Baldridge, K. K.; Hardcastle, K.; Frank, N. L.; Gantzel, P.; Siegel, J. S.; Ziller, J. *Angew. Chem., Int. Ed. Engl.* **1995**, *34*, 1454. (b) Stanger, A. *J. Am. Chem. Soc.* **1998**, *120*, 12034. (c) Review: Shaik, S.; Shurki, A.; Danovich, D.; Hiberty, P. C. *Chem. Rev.* **2001**, *101*, 1501.
(4) Jorgensen, W. L.; Borden, W. T. *J. Am. Chem. Soc.* **1973**, *95*, 6649.
(5) Baldridge, K. K.; Siegel, J. S. *J. Am. Chem. Soc.* **2001**, *123*, 1755.
(6) Shelton, G. R.; Hrovat, D. A.; Wei, H.; Borden, W. T. *J. Am. Chem. Soc.* **2006**, *128*, 12020.
(7) Matsuura, A.; Komatsu, K. *J. Am. Chem. Soc.* **2001**, *123*, 1768.
(8) Eisenstein, F. W. B.; Willis, A. C.; Cullen, W. R.; Soulen, R. L. *J. Chem. Soc., Chem. Commun.* **1981**, 526.

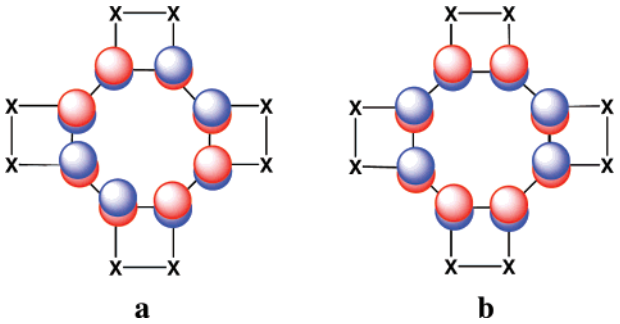

Figure 1. Degenerate e_{2u} NBMOs of D_{8h} COT. Occupancy of NBMO **a** favors exocyclic localization of the π bonds, whereas occupancy of **b** favors endocyclic localization.

tetrafluoroethano group, the in-phase combination is the lowest unoccupied (LU)MO. Therefore, LUMOs of the four tetrafluoroethano annelating groups in **3** have the correct symmetry to accept electrons from the bonding π orbitals of the endocyclic double bonds in **3b**, but not from the highest occupied (HO)MOs of the exocyclic double bonds in **3a**. Consequently, **3b** is favored over **3a**.[5,8]

The calculated preferences for endocyclic double bond localization in tetrakis-annelated COTs **4**−**7**, on which Baldridge and Siegel also performed calculations,[9] can be similarly rationalized based on the local symmetries of the HOMOs and LUMOs of the exocyclic double bonds in **4a**−**7a** and of the endocyclic double bonds in **4b**−**7b**. However, a more rigorous analysis of the abilities of all of the substituents in **2**−**7** to cause either exocyclic or endocyclic localization of the double bonds in the planar, eight-membered rings can be formulated in terms of the pair of COT nonbonding (NB)MOs, shown in Figure 1. At D_{8h} geometries of unsubstituted COT these NBMOs are degenerate by symmetry, and each is effectively occupied by one electron in the lowest singlet state.[10] However, the orbital degeneracy can be lifted by substituents, and in derivatives of COT, such as **2**−**7**, two π electrons will selectively occupy the lower energy of these two MOs.

In **2** and **7**, one linear combination of the HOMOs of each of the four X−X substituents has the same symmetry as that of NBMO **b** in Figure 1, but none of the combinations of substituent HOMOs has the same symmetry as that of NBMO **a**. The interaction between NBMO **b** and a combination of the substituent HOMOs destabilizes **b**, relative to NBMO **a**, and so in **2** and **7** a pair of π electrons goes into NBMO **a**. Consequently, exocyclic localization of the π bonds, as in **2a** and **7a**, is computed to be favored.[5,9]

The calculated preference for endocyclic localization of the double bond in **3**−**6** can be similarly rationalized in terms of the NBMOs in Figure 1. Stabilization of orbital **b** by mixing with one combination of the LUMOs of the substituents in **3**−**5** and destabilization of orbital **a** by mixing with one combination of the HOMOs of the hydrazino substituents in **6** both favor double occupancy of orbital **b**. Consequently, endocyclic localization of the π bonds, as in **3b**−**6b**, is computed to be favored over exocyclic localization, as in **3a**−**6a**.[5,9]

(9) Baldridge, K. K.; Siegel, J. S. *J. Am. Chem. Soc.* **2002**, *124*, 5514.
(10) In the lowest singlet state of D_{8h} COT, one electron occupies each of the disjoint NBMOs that result from taking the sum and difference of the nondisjoint NBMOs in Figure 1. This $^1B_{1g}$ state is lower in energy than the corresponding $^3A_{2g}$ state, so that D_{8h} COT provides a rare example of a violation of Hunds rule. Wenthold, P. G.; Hrovat, D. A.; Borden, W. T.; Lineberger, W. C. *Science* **1996**, *272*, 1456.

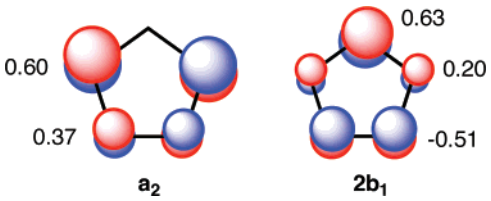

Figure 2. Degenerate e_1'' orbitals of D_{5h} CPD, labeled with the C_{2v} representation to which each belongs. The coefficients of the AOs in the a_2 and $2b_1$ MOs, shown above, are those obtained from simple Hückel theory.

We wondered whether the same types of simple considerations of the symmetries of the HOMOs and LUMOs of substituents would lead to the correct prediction of the localization of the π bonds in the lowest electronic state of annelated cyclopentadienyl (CPD) radicals. The answer to this question is not trivial. Unlike the degenerate e_{2u} NBMOs of COT, shown in Figure 1, the degenerate e_1'' MOs of CPD in Figure 2 each have different coefficients at the same ring carbon atoms. Therefore, in annelated CPD radicals, it is not clear *a priori* whether the symmetries of the HOMOs and LUMOs of the X−X substituents, or the sizes of the coefficients of the degenerate CPD orbitals at the carbons to which the substituents are attached, will determine whether the a_2 MO is doubly occupied and $2b_1$ is singly occupied, or vice versa.

Our computational investigation of this question was motivated by the recent report by Komatsu and co-workers of the X-ray structure of bis-annelated CPD radical **8**.[11] In the crystal the *tert*-butyl group at the fifth carbon has conformation **8a**, in which one of the C−CH_3 bonds of the *tert*-butyl group lies in the molecular plane. This conformation lacks both symmetry elements of the C_{2v} point group that would have allowed a clear distinction between a $^2A_2$ wave function, in which the a_2 CPD MO is singly occupied, and a $^2B_1$ wave function, in which the $2b_1$ CPD MO is singly occupied.

However, Komatsu and co-workers carried out UB3LYP/6-31G(d) calculations on conformations **8b** and **8c** in which one of the C−CH_3 bonds of the *tert*-butyl group lies in a symmetry plane that is perpendicular to the plane of the ring. The calculated bond lengths indicate that the preferred wave function is clearly $^2A''$ (**8b**), rather than $^2A'$ (**8c**).

In this paper we report the results of our UB3LYP/6-31G(d) calculations on a wide variety of mono- and bis-annelated CPD radicals. We find that in some cases the prediction of whether the $^2A_2$ or $^2B_1$ state of these radicals is lower in energy cannot be made on the basis of just the symmetry of the HOMO and/or LUMO of the annelating X−X substituents. Instead, the sizes of the coefficients of the degenerate MOs of the CPD radical at the sites of annelation generally play the dominant role in determining whether $^2A_2$ or $^2B_1$ is the ground state.

Computational Methodology

Calculations based on density functional theory were carried out with the three-parameter functional of Becke and the correlation functional of Lee, Yang, and Parr (B3LYP).[12] Geometries were optimized at the unrestricted UB3LYP level of theory, and UB3LYP vibrational analyses were performed at each stationary point, in order to confirm its identity as a minimum or a transition state. The vibrational frequencies were used, without scaling, to convert energy differences into enthalpy

(11) Kitagawa, T.; Ogawa, K.; Komatsu, K. *J. Am. Chem. Soc.* **2004**, *126*, 9930.
(12) (a) Becke, A. D. *J. Chem. Phys.* **1993**, *98*, 5648. (b) Lee, C.; Yang, W.; Parr, R. G. *Phys. Rev. B* **1998**, *37*, 785.

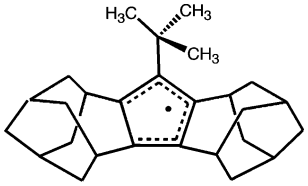

8a

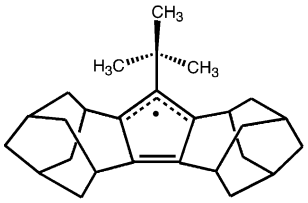

8b

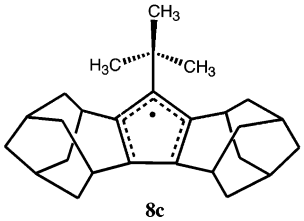

8c

differences at 298 K. All calculations were performed with the 6-31G-(d) basis set[13] using the Gaussian 03 suite of programs.[14] Komatsu and co-workers found that UB3LYP/6-31G(d) calculations predict a geometry for **8** that is in excellent accord with the experimental geometry obtained by X-ray crystallography.[11]

Results and Discussion

Unsubstituted CPD Radical. The partial occupancy of one of the e_1'' MOs of the CPD radical makes the D_{5h} radical subject to Jahn−Teller distortions to lower symmetry.[15] As shown in Figure 3, the Jahn−Teller distortion which arises from placing the unpaired electron in the e_{1x}'' (a_2) MO gives an equilibrium geometry that is best described as being comprised of an allyl radical plus a localized double bond. In contrast, placing the unpaired electron in the e_{1y}'' ($2b_1$) MO gives an equilibrium geometry that is best described as belonging to a pentadienyl radical, with a single bond between the two terminal carbons.

Like previous electronic structure calculations,[16] UB3LYP finds the optimized geometries of the $^2A_2$ and $^2B_1$ states to be nearly isoenergetic. Consequently, by alternately passing between the five equivalent geometries that have $^2A_2$ wave functions and the five that have $^2B_1$ wave functions, the CPD radical is predicted to be able to pseudorotate around a D_{5h} geometry with little or no barrier.[17] In fact, consistent with the prediction of very rapid pseudorotation of CPD radical, the EPR spectrum shows that, on the EPR time scale, the odd electron appears with equal probability on all five carbon atoms.[18]

Mono-annelated CPD Radicals. The results of our calculations on mono-annelation of CPD radical with π-electron donating and π-electron accepting X−X substituents, many of which were considered by Baldridge and Siegel in their studies of bond localization in COT,[5,9] are given in Table 1. The results in this table show that mono-annelation is capable of resulting in very different relative energies for the optimized geometries of the $^2A_2$ and $^2B_1$ states of CPD radicals.

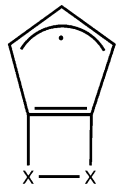

9a, X = CF_2
10a, X = C=O
11a, X = BH
12a, X = CH_2
13a, X = NH
14a, X = $C=CH_2$
15a, X-X = HC=CH

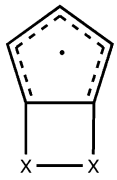

9b, X = CF_2
10b, X = C=O
11b, X = BH
12b, X = CH_2
13b, X = NH
14b, X = $C=CH_2$
15b, X-X = HC=CH

16a, m = n = 1
17a, m = 1, n = 2
18a, m = n= 2

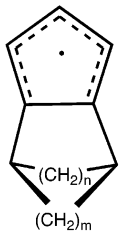

16b, m = n = 1
17b, m = 1, n = 2
18b, m = n= 2

The biggest energy difference, ΔE, between the geometries optimized for the $^2A_2$ and $^2B_1$ wave functions is found in **15**, in which the annelating group is etheno. As shown schematically in Figure 4, in **15** the filled π MO of the etheno group interacts with the $2b_1$ MO of the CPD ring, while the empty π^* MO of the etheno group mixes with the a_2 MO of the CPD ring. The former interaction destabilizes the $2b_1$ MO of the CPD ring, whereas the latter interaction stabilizes the a_2 MO. Therefore, the lowest energy state of **15** is $^2B_1$, in which two electrons occupy a_2 and only one electron occupies $2b_1$.

The HOMO of the 1,3-bridged cyclobutane ring in **16**, like the filled etheno π orbital in **15**, has b_1 symmetry.[4] Mixing of the HOMO of the cyclobutane ring in **16** with the $2b_1$ π MO of the CPD ring destabilizes $2b_1$ and favors the $^2B_1$ state over the $^2A_2$ state. However, ΔE between **16a** and **16b** is calculated to be only about one-third as large as that between **15a** and **15b**.

There are at least three reasons why the size of the energetic preference for **16b** over **16a** is only a fraction of the size of the preference for **15b** over **15a**. First, the b_1 HOMO of the 1,3-bridged, four-membered ring in **16** is spread over all four carbons,[4] rather than being localized to just the two carbons

(13) Hariharan, P. C.; Pople, J. A. *Theor. Chim. Acta* **1973**, *28*, 213.
(14) Frisch, M. J., et al. *Gaussian 03*, revision C.02; Gaussian, Inc.: Wallingford, CT, 2004.
(15) Jahn, H. A.; Teller, E. *Proc. R. Soc. London, Ser. A* **1937**, *161*, 220.
(16) (a) Borden, W. T.; Davidson, E. R. *J. Am. Chem. Soc.* **1979**, *101*, 3771. (b) Ha, T.-K., Meyer, R.; Günthard, H. H. *Chem. Phys. Lett.* **1980**, *69*, 510. (c) Bearpark, M. J.; Robb, M. A.; Yamamoto, N. *Spectrochim. Acta, Part A* **1999**, *55*, 639. (d) Applegate, B. E.; Miller, T. A.; Barckholtz, T. A. *J. Chem. Phys.* **2001**, *114*, 4855. (e) Zilberg, S.; Haas, Y. J. *Am. Chem. Soc.* **2002**, *124*, 10683.
(17) Liehr, A. D. *J. Phys. Chem.* **1963**, *67*, 389.
(18) (a) Liebling, G. R.; McConnell, H. M. *J. Chem. Phys.* **1965**, *42*, 3931. (b) The electronic spectrum of the radical has also been obtained, and the vibrational structure has been interpreted. Applegate, B. E.; Bezant, A. J.; Miller, T. A. *J. Chem. Phys.* **2001**, *114*, 4869.

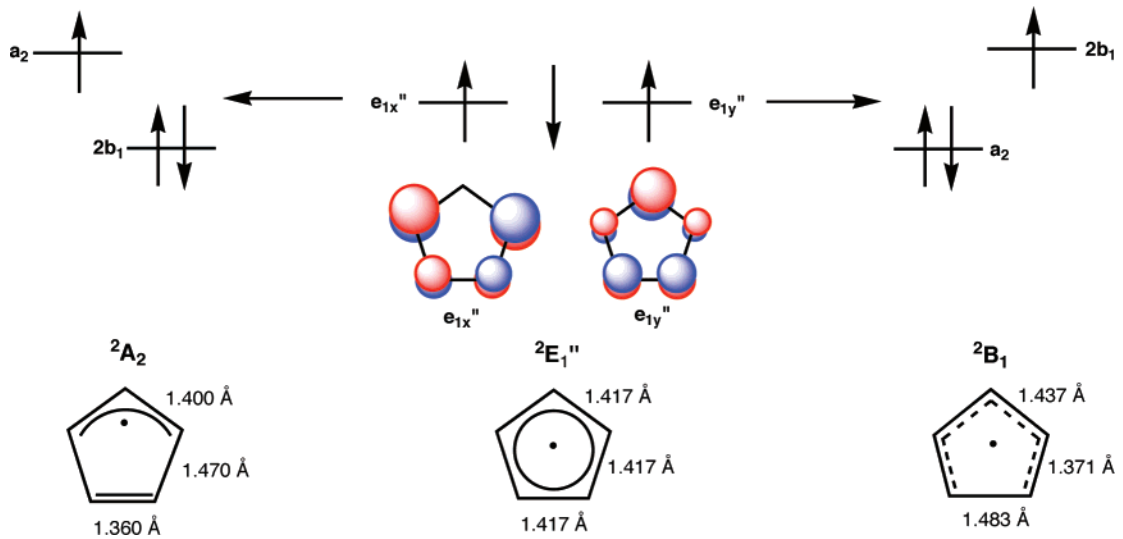

Figure 3. Schematic depiction of the effect of the e_{2y}' component of the first-order, Jahn−Teller distortion on the energies of the e_{1x}'' (a_2) and e_{1y}'' (b_1) MOs of the cyclopentadienyl radical, The UB3LYP/6-31G(d) optimized, C−C bond lengths in the $^2A_2$ and $^2B_1$ states that result from the opposite phases of this distortion are shown. At their respective, optimized geometries these two states are calculated to have essentially the same energy.

Table 1. Lower Energy Geometry (LEG, **a** or **b**)[a] in Mono-annelated CPD Radicals **9**−**21** and the Energy Difference (ΔE, kcal/mol) between the Lower Energy Geometry and the Higher Energy Geometry

LEG	9a	10a	11a	12b	13b	14b	15b	16b	17b	18b	19a	20b	21a
ΔE	4.1	6.6[b]	16.7[c]	3.5	8.9[d]	5.9	38.1	13.0	6.6	4.4	3.7[c]	18.7[d]	21.0

[a] In C_{2v} symmetry geometries of type **a** have $^2A_2$ wave functions, and geometries of type **b** have $^2B_1$ wave functions. [b] In C_{2v} symmetry the lowest electronic state is $^2A_1$, in which an electron is removed from the in-phase combination of lone-pair orbitals on the carbonyl groups and transferred to the singly occupied π MO. [c] Borons constrained to be planar, as in ref 9. When the symmetry of **11** is reduced to C_2, the energy of **11a** goes down by 3.0 kcal/mol, but the energy of **11b** is unaffected. When the symmetry of **19** is reduced to C_s, the energies of **19a** and **19b** go down by, respectively, 1.4 and 0.3 kcal/mol. [d] Calculations performed in C_2 symmetry with the nitrogens pyramidalized *trans* to each other.

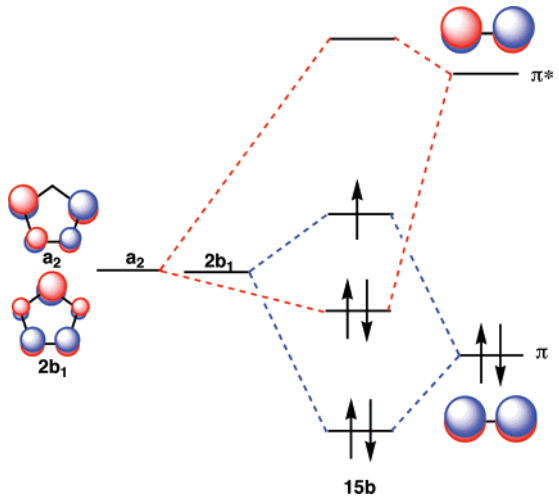

Figure 4. Orbital interaction diagram for **15**, showing why mixing of the a_2 and $2b_1$ π orbitals of the CPD radical with the π and π^* orbitals of the annelated etheno group strongly favors the $^2B_1$ state, in which a_2 is doubly occupied and $2b_1$ is singly occupied.

that are connected to the CPD ring, as is the case in **15**. Second, the HOMO-1 of the 1,3-bridged cyclobutane ring in **16** has a_2 symmetry and, thus, interacts with the a_2 MO of the CPD ring. This interaction with a lower-lying, filled orbital raises the energy of a_2. Finally, the cyclobutane ring in **16** lacks the empty π^* orbital of the etheno group in **15**, and the absence in **16** of the stabilizing interaction between a low-lying, empty, substituent orbital and the a_2 MO of the CPD ring also contributes to making the energy difference between $2b_1$ and a_2 much smaller in **16** than in **15**.

As the size of the saturated ring increases from four to five to six carbons in **16**−**18**, the dominant interaction remains that between a b_1 MO of the ring[4,19] and the $2b_1$ CPD MO. Therefore, the $^2B_1$ electronic wave functions of **16b**−**18b** are all calculated to be lower in energy than the $^2A_2$ wave functions **16a**−**18a**. However, as the size of the saturated ring increases, the highest b_1 MO of the ring is progressively spread over more carbons than just the two that are attached to the CPD ring; and, in addition, the energy difference between the highest b_1 and a_2 ring orbitals decreases with increasing ring size. These two factors both contribute to the calculated decrease in ΔE on going from **16** to **17** to **18**.

The calculated preference for equilibrium geometries **9a**−**11a**, which have $^2A_2$ wave functions, over **9b**−**11b**, which have $^2B_1$ wave functions, can also be readily understood on the basis of the symmetry of the relevant frontier MO of the X−X groups in these molecules. X = CF_2, C=O, and BH each have a low-lying, unfilled orbital that can act as a π electron acceptor. When the unfilled π or π-like orbitals of two such X groups interact with each other, the in-phase ($n_+ = b_1$) combination of these π acceptor orbitals is lower in energy than the out-of-phase ($n_- = a_2$) combination. Consequently, as shown schematically in Figure 5 for **11** (X = BH), the X−X substituents in **9**−**11** provide more stabilization for the $2b_1$ π MO of CPD than for the a_2 MO. Therefore, in the ground state of each of these three radicals the $2b_1$ MO of CPD is doubly occupied and the a_2 CPD MO is singly occupied, making the ground state $^2A_2$.

(19) See, for example, the depictions in Jorgensen, W. L.; Salem, L. *The Organic Chemists Book of Orbitals;* Academic Press: New York, 1973.

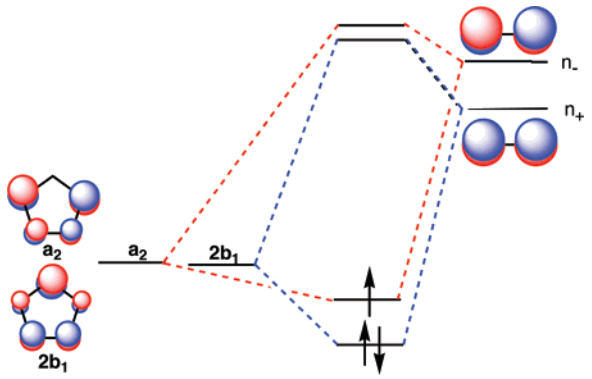

Figure 5. Schematic orbital interaction diagram, showing why, based on the relative energies of the n_+ and n_- combinations of the empty, electron-accepting orbitals on boron, $^2A_2$ is expected to be the ground state of **11** (X = BH).

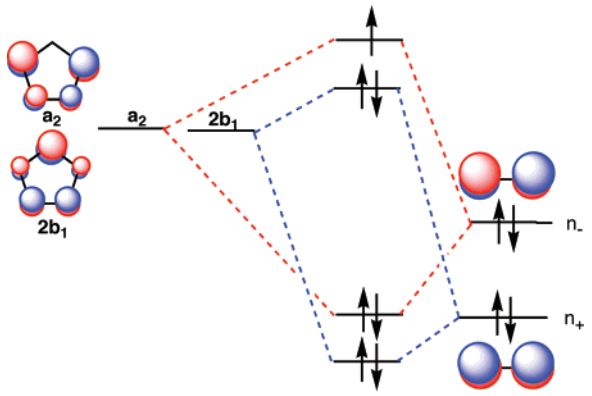

Figure 6. Schematic orbital interaction diagram, showing why, based on the relative energies of the n_+ and n_- combinations of the electron-donating, lone pair orbitals in **13** (X = NH), $^2A_2$ might be expected to be the ground state of **13**. However, as shown by the computational results in Table 1, the prediction of a $^2A_2$ ground state for **13** is incorrect.

The foregoing discussion shows that the results in Table 1 are easy to understand on the basis of (a) the symmetries of the LUMOs of the π electron accepting X−X substituents in **9**−**11**, (b) the symmetries of the HOMOs of the π electron donating X−X substituents in **16**−**18**, and (c) the symmetries of both the HOMO and the LUMO of the π bond in the etheno group in **15**. However, the results of the calculations on **12**−**14** cannot be understood on the basis of the symmetries of the HOMOs of the electron-donating substituents in these three radicals.

When the filled π or π-like orbitals of two electron donating substituents, such as X = CH_2, NH, and C=CH_2, interact with each other, the out-of-phase ($n_- = a_2$) combination is higher in energy than the in-phase ($n_+ = b_1$) combination. Therefore, the HOMOs of the π donating, X−X substituents in **12**−**14** all have a_2 symmetry. Consequently, as shown schematically in Figure 6 for **13** (X = NH), frontier orbital theory predicts that mixing with the filled π orbitals of the X−X substituents in **12**−**14** should destabilize the a_2 MO of CPD by more than the $2b_1$ MO. Thus, the $^2A_2$ wave functions of **12a**−**14a** should be lower in energy than the $^2B_1$ wave functions of **12b**−**14b**.

However, Table 1 shows the opposite to be the case. Moreover, the amount of energy by which **12b**−**14b** are favored over **12a**−**14a** is not trivial. For example, **13b** is computed to be lower than **13a** by ΔE = 8.9 kcal/mol.

Why do the predictions of the ground states of **12**−**14**, based on the relative energies of the filled a_2 and b_1 MOs of the substituents, fail? In order to answer this question, it is useful to consider explicitly the expression for the energy change that arises from the mixing of a zeroth-order orbital, ψ_{i0}, with all the other zeroth-order orbitals, ψ_{j0}, of the same symmetry. Using second-order perturbation theory, the energy change, ΔE_i, in ψ_{i0} that is caused by mixing with all the ψ_{j0} is given by

$$\Delta E_i = \sum_{i \neq j} (\int \psi_{i0} H' \psi_{j0})^2 / (E_{i0} - E_{j0}) \qquad (1)$$

where H′ is the perturbation that causes ψ_{i0} and ψ_{j0} to mix, $\int \psi_{i0} H' \psi_{j0}$ is the energy of their interaction, and $E_{i0} - E_{j0}$ is the energy difference between the zeroth-order MOs that are mixed.

According to eq 1, ΔE_i depends not only on the size of $E_{i0} - E_{j0}$ but also upon the size of $\int \psi_{i0} H' \psi_{j0}$. Therefore, although predictions of the relative sizes of the energy changes that occur on orbital mixing can often be made by comparing the relative sizes of the orbital energy differences in the denominator of eq 1, the relative sizes of the interaction energies in the numerator can also play an important role. The coefficients in Figure 2 of the AOs in the a_2 and $2b_1$ MOs of CPD show that the values of $(\int \psi_{i0} H' \psi_{j0})^2$ are not the same for the interactions of these two MOs with the n_+ and n_- combinations of either the empty boron AOs in **11** or the nitrogen lone pair AOs in **13**. Based on the AO coefficients at the two ring atoms to which the substituents are attached, the numerator of eq 1 is a factor of $(0.51/0.37)^2 = 1.9$ larger for interactions involving the $2b_1$ MO than for interactions involving the a_2 MO.

Therefore, for the stabilizing interactions with the π electron accepting boron substituents in **11**, the numerator of eq 1 favors double occupancy for $2b_1$ and single occupancy for a_2. Consequently, both the numerator and the denominator of eq 1 favor single occupancy of the a_2 MO in **11**, as well as in **9** and **10**, in which the substituents are also π acceptors.

However, the situation for the π donor substituents in **12**−**14** is different from the situation for the π acceptor substituents in **9**−**11**. As shown schematically in Figure 6 for **13**, the energy difference in the denominator of eq 1 favors single occupancy of a_2. In contrast, the interaction energies in the numerator favor single occupancy of $2b_1$. The results in Table 1 show that the effect of the numerator of eq 1 clearly dominates the effect of the denominator in determining the ground states of **12**−**14**.

Inserting a methylene group between the two substituents, X, in **9**−**14** should make the energies of the n_+ and n_- combinations of the substituent orbitals more nearly equal.[20] Thus, CH_2 insertion should make the energy differences in the denominator of eq 1 more nearly equal for the interaction of the a_2 CPD orbital with the n_- combination of substituent orbitals and for the interaction of $2b_1$ with n_+. More nearly equal denominators for the interactions with the n_- and n_+ combinations of the electron-accepting BH π orbitals should provide less stabilization for the $2b_1$, relative to the a_2 CPD MO, in **19** than in **11.** Consequently, ΔE between **19a** and **19b** should be smaller than ΔE between **11a** and **11b**.

(20) Inserting a CH_2 group between the borons in **11** and the nitrogens in **13** does more than just equalize the energies of the n_+ and n_- combinations. Since the n_+ combinations of substituent AOs interact with the π donating CH_2 group, but the n_- combinations do not, the CH_2 group actually reverses the relative energies of n_+ and n_-.

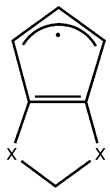

19a, X = BH
20a, X = NH

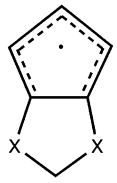

19b, X = BH
20b, X = NH

21a

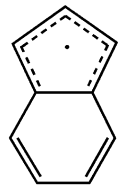

21b

On the other hand, more nearly equal denominators for the interactions with the n_- and n_+ combinations of the electron-donating NH orbitals in **20** than in **13** should provide less destabilization of the a_2, relative to the $2b_1$ CPD MO in **20** than in **13**. Therefore, ΔE between **20b** and **20a** should be larger than ΔE between **13b** and **13a**.

The results of our calculations on radicals **19** and **20** in Table 1 are in accord with these expectations as to what should happen when the energy denominators in eq 1 for the a_2 and b_1 interactions become more nearly equal in size than in the case of **11** and **13**.[20] $\Delta E = 3.7$ kcal/mol between **19a** and **19b** is 13.0 kcal/mol smaller than $\Delta E = 16.7$ kcal/mol between **11a** and **11b**, and $\Delta E = 18.7$ kcal/mol between **20a** and **20b** is 9.8 kcal/mol larger than $\Delta E = 8.9$ kcal/mol between **13a** and **13b**.

In contrast to the effect of inserting a CH_2 group in **11** and **13**, changing the mode of attachment of the butadiene substituent in **14** to that in **21** affects the numerator of eq 1 while holding the denominator constant. As shown schematically in Figure 7, the HOMO (ψ_2) of butadiene, has larger coefficients at the terminal carbons, which are attached to the CPD ring in **21**, than those at the central carbons, which are the points of attachment in **14**. Thus, the mixing of the butadiene HOMO, which has a_2 symmetry, with the CPD MO of the same symmetry results in a much higher-lying a_2 MO in **21** than in **14**.

The LUMO (ψ_3) of butadiene also has much larger coefficients at the terminal carbons than those at the central carbons, but the reverse is true of the lowest energy π MO (ψ_1) of butadiene. Mixing with ψ_3 lowers the energy of the $2b_1$ MO of CPD, and mixing with ψ_1 raises the energy of $2b_1$. Consequently, as shown in Figure 7, mixing of ψ_1 and ψ_3 of butadiene with the $2b_1$ CPD MO results in a much lower-lying $2b_1$ frontier MO in **21** than that in **14**.

As a consequence of these changes in the energies of the perturbed a_2 and $2b_1$ MOs, singly occupying the former and doubly occupying the latter should be much more favorable in the case of **21** than in **14**. In fact, our UB3LYP/6-31G(d) calculations predict that **21a** is lower in energy than **21b** by $\Delta E = 21.0$ kcal/mol, whereas the same type of calculations find that **14b** is lower than **14a** by $\Delta E = 5.9$ kcal/mol.[21] Thus, changing the mode of attachment of the butadiene substituent in **14** to that in **21** results in a calculated change of 26.9 kcal/mol in the relative energies of the $^2B_1$ and $^2A_2$ states.

Bis-annelated CPD Radicals. In addition to performing UB3LYP calculations on mono-annelated CPD radicals **9**−**21**, we also carried out UB3LYP calculations on bis-annelated radicals **22**−**30**. The results of the latter calculations are given in Table 2. Symmetry has less effect on the orbital interactions

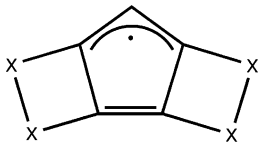

22a, X = CF_2
23a, X = C=O
24a, X = BH
25a, X = CH_2
26a, X = NH
27a, X = $C=CH_2$
28a, X-X = HC=CH
29a, X-X = $HC(CH_2)_2CH$
30a, X-X = HC=CH-CH=CH

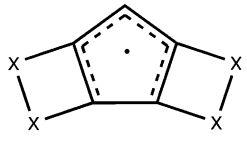

22b, X = CF_2
23b, X = C=O
24b, X = BH
25b, X = CH_2
26b, X = NH
27b, X = $C=CH_2$
28b, X-X = HC=CH
29b, X-X = $HC(CH_2)_2CH$
30b, X-X = HC=CH-CH=CH

in the bis-annelated CPD radicals than on their mono-annelated counterparts. Unlike the case in **9**−**21**, in **22**−**30** the symmetry elements do not pass through the X−X bonds. Consequently, in **22**−**30** the in-phase and out-of-phase combinations of 2p-π AOs on each X−X group mix with both the a_2 and the $2b_1$ CPD MOs.

Nevertheless, the $2b_1$ CPD MO has a node between the pair of carbons to which each X−X group is attached in the bis-annelated radicals, whereas the a_2 MO does not. Therefore, in **22**−**30** n_+, the in-phase combination of 2p-π AOs on each X−X group, mixes predominantly with the a_2 CPD MO; and n_-, the out-of-phase combination of these AOs, mixes predominantly with $2b_1$. This is the reverse of the mixing pattern in mono-annelated radicals **9**−**21**.

Also in reverse of the situation in **9**−**21**, in **22**−**30** the a_2 MO has larger coefficients than the $2b_1$ MO at the pairs of atoms to which each of the X−X groups is attached. Therefore, it is easy to predict that the symmetry of the ground state wave function of each bis-annelated CPD radical **22**−**30** should be reversed from that of the corresponding mono-annelated CPD radical **9**−**16** and **21**.

Since there are twice as many X−X groups in **22**−**30** as those in **9**−**21**, it is also easy to predict that ΔE, the size of the energy difference between the equilibrium geometries that are associated with the $^2A_2$ and $^2B_1$ wave functions, should be substantially larger in the bis-annelated than in the mono-annelated CPD radicals. However, as already noted, in **22**−**30** there is some mixing of n_+ with $2b_1$ and of n_- with a_2. Consequently, ΔE in each bis-annelated radical is expected to be less than a factor of 2 larger than ΔE in its mono-annelated counterpart.

Comparison of the results in Table 2 with those in Table 1 shows the extent to which the above predictions are confirmed. For each set of substituents, X−X, the lowest energy wave function and the associated equilibrium geometry of **22**−**30** are, indeed, reversed from those of **9**−**16** and **21**. In addition, except for **26** and **28**, ΔE is, in fact, about 50% larger in each bis-annelated CPD radical than in its mono-annelated counterpart.

(21) Hückel theory not only correctly predicts the change from a $^2B_1$ ground state in **14** to a $^2A_2$ ground state in **21** but also correctly predicts that the energy difference between the singly occupied MO and the doubly occupied MO of lower energy is much larger in **21** than in **14**. A version of Figure 7, giving the Hückel energies of the MOs, is available in the Supporting Information for this paper.

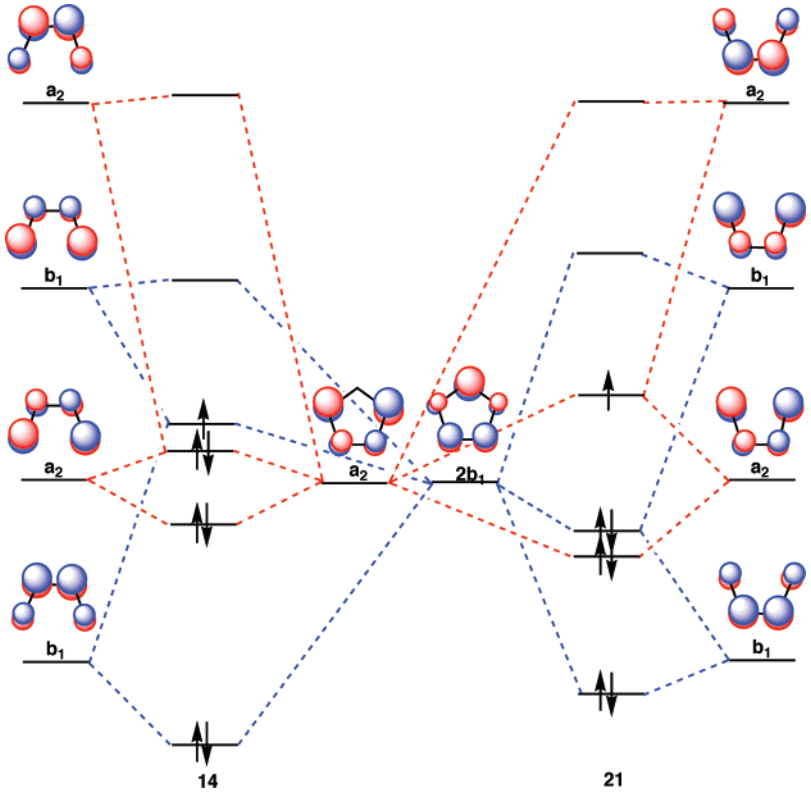

Figure 7. Qualitative orbital interaction diagrams for mixing between the degenerate, bonding, π MOs of CPD radical and the π MOs of 1,3-butadiene when C2 and C3 of butadiene are attached to CPD in **14**, and when C1 and C4 of butadiene are attached to CPD in **21**. The red dotted lines represent the effects of interactions between a_2 MOs, and the blue dotted lines represent the effects of interactions between b_1 MOs.

Table 2. Lowest Energy Geometry (LEG, **a** or **b**)[a] in Bis-annelated CPD Radicals **22**−**30** and the Energy Difference (ΔE, kcal/mol) between the LEG and the Higher Energy Geometry

LEG	22b	23b	24b	25a	26a	27a	28a	29a	30b
ΔE	6.2	9.0[b]	24.3[c]	4.9	4.4[d]	7.1	34.2	19.2	29.5

[a] In C_{2v} symmetry geometries of type **a** have $^2A_2$ wave functions, and geometries of type **b** have $^2B_1$ wave functions. [b] In C_{2v} symmetry the lowest electronic state is $^2B_2$, in which an electron is removed from a b_2 combination of lone-pair orbitals on the carbonyl groups and transferred to the singly occupied π MO. [c] Borons constrained to be planar, as in ref 9. When the structure of **24b** is reoptimized in C_2 and in C_s symmetry, its energy is lowered by, respectively, 8.4 and 6.7 kcal/mol. [d] Calculations performed in C_2 symmetry with the lone pairs on nitrogen pyramidalized *trans* to each other.

The reason why ΔE in **26** is actually about 50% smaller, rather than 50% larger, than ΔE in **13** is revealed by Figure 8. The partial double bonds in **26b**, which is the higher energy geometry of **26**, are strongly pyramidalized *anti* to each other. In contrast, **26a** has nearly planar carbons, as do both **13a** and **13b**.

Pyramidalization presumably occurs in **26b** because, on transferring an electron from the $2b_1$ MO of the CPD ring in **26a** into the a_2 MO in **26b**, the bonding π interaction between the pair of symmetry-related, adjacent carbons in the former MO is replaced by the antibonding interaction in the latter MO. *anti*-Pyramidalization of these two carbons in **26b** reduces the π overlap between them and thus minimizes the energetic effect of the excitation of an electron from $2b_1$ to a_2.

anti-Pyramidalization of the symmetry-related, adjacent carbons in **26b** can only occur in C_2 symmetry. In C_s symmetry pyramidalization would have to be *syn*, and *syn* pyramidalization should be less effective than *anti* at reducing the overlap between

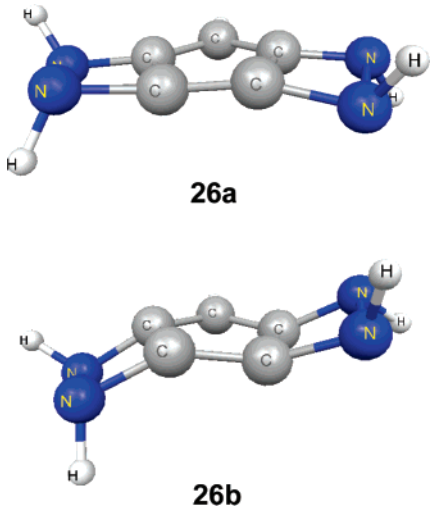

Figure 8. Optimized geometries calculated for **26a** and **26b**.

these two carbons. In fact, in C_s symmetry pyramidalization does not occur in **26b**, and $\Delta E = 11.9$ kcal/mol between **26b** and **26a**. This value of ΔE is 34% larger than the value of $\Delta E = 8.9$ kcal/mol between **13a** and **13b**. Thus, *anti*-pyramidalization of the double bonds in **26b** is, indeed, responsible for the smaller than expected energy difference between the lowest energy geometries of **26b** and **26a**.

The reason why ΔE for **28** in Table 2 is actually smaller than ΔE for **15** in Table 1, rather than being ca. 50% larger, has a different origin. Both the bonding $1a_2$ and the antibonding $2a_2$* MOs of the CPD ring mix with the $\pi_1-\pi_2$ and π_1*$-\pi_2$* orbitals of the two annelated etheno groups. However, the match of the nodal pattern of $1a_2$ with that of $\pi_1-\pi_2$ and of

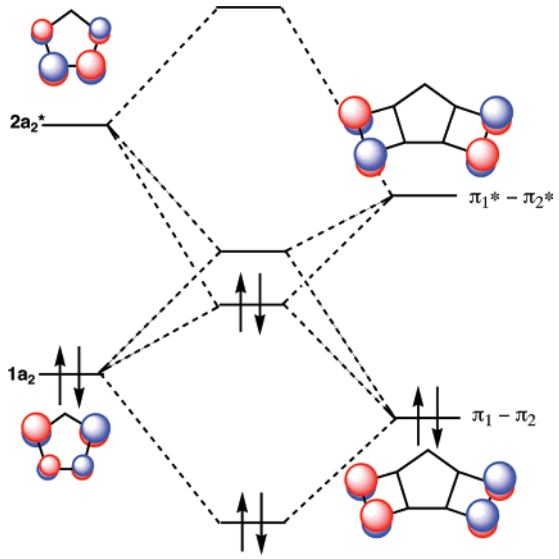

Figure 9. Schematic orbital interaction diagram, showing that the $1a_2$ and $2a_2$* MOs of the CPD ring and the $\pi_1-\pi_2$ and $\pi_1^*-\pi_2^*$ orbitals of the two annelating etheno groups all contribute strongly to the second lowest a_2 orbital of **28**.

the nodal pattern of $2a_2$* with that of $\pi_1^*-\pi_2^*$ makes the interactions between these pairs of orbitals strongest. As indicated in Figure 9, the strongly destabilizing interaction between $1a_2$ and $\pi_1-\pi_2$ and the strongly stabilizing interaction between $2a_2$* and $\pi_1^*-\pi_2^*$ results in the latter pair of orbitals being mixed strongly into the second lowest of the a_2 MOs of **28**, despite the fact that $2a_2$* and $\pi_1^*-\pi_2^*$ are both antibonding orbitals.[22]

The stabilizing interaction between the antibonding $2a_2$* CPD orbital and the a_2 combination of the π* orbitals of the annelated etheno groups makes the energy of the second a_2 MO of **28** much lower than it would have been had it consisted only of $1a_2$ mixing in an antibonding fashion with $\pi_1-\pi_2$. In contrast, the second b_1 MO of **15** consists only of the $2b_1$ CPD orbital interacting in an antibonding fashion with the π orbital of the annelated etheno group. Consequently, ΔE in Table 2 for the $b_1 \rightarrow a_2$ excitation in **28a** → **28b** is smaller than ΔE in Table 1 for the $a_2 \rightarrow b_1$ excitation in **15b** → **15a**.

Other Perspectives. In order to understand the results of our calculations on whether each of the radicals **9**−**30** has a $^2A_2$ or a $^2B_1$ ground state, we have analyzed the orbital interactions between the degenerate MOs of the parent CPD radical and the HOMOs and LUMOs of various substituents. However, just as there are multiple ways of understanding the preference for exocyclic versus endocyclic localization of the double bonds in the COT rings of **2**−**7**, other perspectives can be used to understand and/or predict the ground states ($^2A_2$ or $^2B_1$) of **9**−**30**.

For example, the depictions in Figure 3 of the bonding in the two lowest-lying states of CPD radical show that in the $^2A_2$ state of **15** a π bond is largely localized at the two carbons to which the etheno group is attached. Thus, **15a** contains a cyclobutadiene ring, whereas **15b** does not; so the Hückel 4n + 2 rule correctly predicts that **15b** should be substantially favored over **15a**.

Similarly, in **28b** π bonds are largely localized at the two sets of carbons to which the pair of etheno groups is attached. Application of the Hückel 4n + 2 rule again predicts that **28a** should be favored over **28b**, as it is, in fact, computed to be.

On the other hand, without understanding that the $2a_2$* MO of CPD and the π* MOs of the etheno groups are heavily mixed into the second a_2 MO of **28** (Figure 9), it is not obvious why the calculated bond lengths for **28b** (Figure 10a) are unlike those in the $^2B_1$ state of the parent CPD (Figure 3) and unlike those in the $^2B_1$ state of any of the other CPD radicals on which we have performed calculations.

It certainly could be argued that the structures shown in Figure 10b and c represent two possible ways of arranging the double bonds in the cyclobutadiene rings of **28b**. However, without an orbital interaction diagram, like that in Figure 9, it is not easy to understand why, according to the bond lengths in Figure 10a, the structure shown in Figure 10b provides a much better representation of the bonding in **28b** than the structure shown in Figure 10c.

The positions of the partial double bonds in Figure 3, combined with the Hückel 4n + 2 rule, also predict correctly that **21a** and **30b** should be lower in energy than, respectively, **21b** and **30a**, due to the presence of one benzene ring in **21a** and two in **30b**. However, when C2 and C3 of butadiene, rather than C1 and C4, are annelated to CPD, the Hückel 4n + 2 rule is not useful for predicting the reversal of the ordering of the $^2A_2$ and $^2B_1$ states, which favors **14b** over **14a** and **27a** over **27b**.

It could be assumed that the ground states of **14** and **27** are determined by which type of wave function, $^2A_2$ or $^2B_1$, provides the most delocalization for the unpaired electron. However, in order to explain the reversal in **21** and **30** of the state orderings in **14** and **27**, it must then be assumed that maximum delocalization of the unpaired electron in **14** and **27** is trumped by aromaticity in **21** and **30**.

We believe that the change in the coefficients of the butadiene AOs at the carbons that are attached to the CPD ring on going from **14** to **21** (Figure 7) and on going from **27** to **30** provides a more satisfactory way of explaining the difference between the ground states of each of these pairs of radicals.

Methyl Group Conformations. In addition to being useful for predicting the ground states of those radicals (**15**, **21**, **28**, and **30**) to which the Hückel 4n + 2 rule can be applied, consideration of the positions of the partial double bonds in the $^2A_2$ and $^2B_1$ states of the CPD radical is also very useful for understanding why the preferred conformations of the methyl substituents in **31**−**33** differ between the $^2A_2$ and $^2B_1$ electronic states. For example, our calculations find that the methyl conformation shown in **31a** is favored over that in **31a′** for the $^2A_2$ state of **31**; whereas, the methyl conformation in **31b** is favored over that in **31b′** for the $^2B_1$ state.

The origin of this change in preferred methyl conformations is that minimization of the antibonding interactions between a double bond and the out-of-plane C−H bonds of an allylic methyl group leads to a preference for a methyl conformation in which one C−H bond eclipses the C−C σ bond between the doubly bonded carbons.[23] Thus, in **31**−**33** the preferred methyl group conformation depends on where the partial double bonds are more highly localized, and, as shown in Figure 3, this differs between the $^2A_2$ and $^2B_1$ states.

(22) Summing the orbitals with the phases shown in Figure 9 correctly predicts the a_2 SOMO of **28a** to be a largely nonbonding π orbital, resembling the SOMO of a hepatrienyl radical.

(23) (a) Lowe, J. P. *J. Am. Chem. Soc.* **1970**, *92*, 3799. (b) Hehre, W. J.; Salem. L. *J. Chem. Soc., Chem. Commun.* **1973**, 754. (c) Hehre, W. J.; Pople, J. A.; Devaquet, A. J. P. *J. Am. Chem. Soc.* **1976**, *98*, 664.

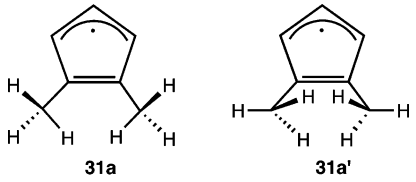

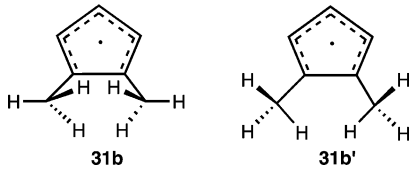

The methyl group orientation shown in **31a** is favored for the $^2A_2$ state by partial localization of a π bond between the substituted carbons in this state. In $^2A_2$ the methyl group conformation shown in **31a** is computed to be 1.4 kcal/mol lower in energy than that in **31a′**, and the latter conformation is found to have three imaginary frequencies. On the other hand, the small amount of π bonding between the substituted carbons in the $^2B_1$ state leads to the methyl group conformation shown in **31b** being computed to be favored in this electronic state by 2.7 kcal/mol over the conformation shown in **31b′**. The methyl group conformation in **31b′** also has three imaginary frequencies in the $^2B_1$ state.

The larger coefficients at the methyl-substituted ring carbons of the $2b_1$ than of the a_2 CPD MO in **31** leads to single occupancy of the $2b_1$ MO being expected to be favored over single occupancy of the a_2 MO. Indeed, our calculations do find **31b** to be lower in energy than **31a** by 2.5 kcal/mol. However, if the methyl group orientation in the $^2B_1$ state is forced to be that shown in **31b′**, which is the orientation preferred in **31a**, the $^2A_2$ state is calculated to be lower in energy than the $^2B_1$ state of **31** by $2.7 - 2.5 = 0.2$ kcal/mol.

The effects of moving the pair of methyl groups in **31** to nonadjacent carbons, as in **32**, are easily predicted. The location of the partial double bonds in the $^2A_2$ state should favor the methyl conformation in **32a** over that in **32a′**. The partial double bonds in the $^2B_1$ state are more delocalized than those in the $^2A_2$ state, but the bond lengths in Figure 3 for the $^2B_1$ state of the unsubstituted radical indicate that the π bond localization shown in **32b** is slightly favored in the $^2B_1$ state. Therefore, in the $^2B_1$ state the methyl conformation shown in **32b** should be weakly favored over that shown in **32b′**. Finally, the much larger coefficients at the substituted carbons of **32** in the a_2 than in the $2b_1$ CPD MO should make $^2A_2$ the ground state by a wide margin.

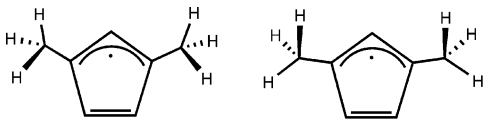

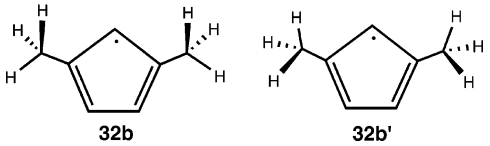

Our calculations confirmed all these predictions. The energy difference between **32a** and **32b** is computed to amount to 5.1 kcal/mol. For the $^2A_2$ state the methyl conformation in **32a** is favored over that in **32a′** by 1.4 kcal/mol, but for the $^2B_1$ state the methyl conformation in **32b** is favored over that in **32b′** by only 0.2 kcal/mol.

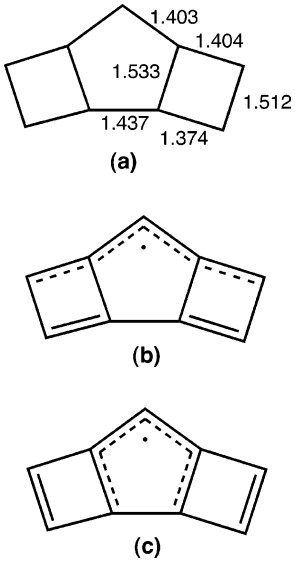

Figure 10. (a) B3LYP/6-31G(d) C−C bond lengths (Å) calculated for **28b**. (b and c) Two possible electronic structures for **28b**.

The results for **31** and **32** make it easy to predict that the methyl conformation shown in **33a** should be favored for the $^2A_2$ state, whereas the methyl conformation in **33b** should be favored for $^2B_1$. These predictions were, indeed, confirmed by our calculations of the energies of both states for all four of the possible conformations of the four methyl groups in **33** that maintain C_{2v} symmetry (see the Supporting Information for details).

Combining the results for **31** and **32**, it is also easy to predict that **33a** should be favored over **33b** by $5.1 - 2.5 = 2.6$ kcal/mol. The actual difference in energy is computed to be 3.5 kcal/mol. The 0.9 kcal/mol discrepancy is likely due to the one additional, nonbonded interaction between the in-plane hydrogens in **33b** than in **33a**.

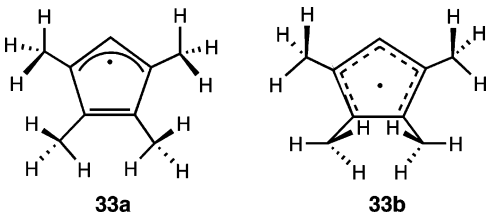

Conclusions

As in planar COT, substituents in CPD radicals have a profound effect on determining the mode of localization of the π bonding. In COT the degenerate NBMOs both have equal coefficients at all the carbons of the ring. Therefore, the symmetries of the highest electron-donating and/or lowest electron-accepting π orbitals of the substituents are the main factor that determines whether localization of the COT π bonds occurs exocyclic or endocyclic to the rings formed by annelation.[24]

In contrast, in CPD the degenerate MOs do not have the same coefficients at all of the atoms of the ring. Consequently, in addition to the symmetries of the HOMOs and/or LUMOs of

the substituents, the sizes of the coefficients of the CPD MOs at the atoms to which the substituents are attached play a role in determining whether the ground state of each annelated CPD radical is $^2A_2$ or $^2B_1$. In some cases (e.g., **9**−**11**, **15**−**18**) both orbital symmetry and coefficient size predict the same ground state. However, in those cases (e.g., **12**−**14**) where orbital symmetry and coefficient size make opposite predictions, our calculations find that coefficient size dominates and that $^2B_1$ is predicted to be the ground state.

An apparent exception to this rule—that the CDP MO coefficient size is more important than the symmetry of the HOMO and/or LUMO of the substituent in determining the ground state—is provided by **21**. In both **14** and **21** 1,3-butadieno is the annelating group, so the symmetries and energies of the orbitals of the substituent are the same in both CPD radicals. Nevertheless, **14** is calculated to have a $^2B_1$ ground state, whereas the ground state of **21** is unequivocally predicted by our calculations to be $^2A_2$. The difference between the ground states of these two radicals is due to the change in the sizes of coefficients at the atoms of the substituents that are attached to the carbons of the CPD ring, when the annelating carbons of 1,3-butadieno change from C2 and C3 in **14** to C1 and C4 in **21**.

In the bis-annelated CPD radicals the symmetry of the ground state is predicted to be reversed from that in the corresponding mono-annelated radicals. In addition, ΔE between the $^2A_2$ and $^2B_1$ states is expected to be larger in a bis-annelated than in the corresponding mono-annelated CPD radicals. In fact, in most cases the calculated energy difference between $^2A_2$ and $^2B_1$ is computed to be about 50% larger in magnitude in the bis-annelated than in the mono-annelated radicals.

Exceptions are provided by **26** and **28**. In the former radical *anti*-pyramidalization of the carbons in the $^2B_1$ excited state reduces the energy difference between this state and the $^2A_2$ ground state. In the latter radical the $1a_2$ and the $2a_2$* CPD orbitals are strongly mixed, and the resulting a_2 MO is stabilized. This a_2 MO is singly occupied in the $^2A_2$ ground state but doubly occupied in the $^2B_1$ excited state, so the excited state profits more than the ground state from the stabilization of this a_2 MO of **28**.

When methyl groups are attached to a CPD radical, the ground state is largely determined by the coefficients of the a_2 and b_1 MOs at the carbons to which the methyl groups are attached. However, the conformations of the methyl groups play a role in the sizes of the $^2A_2 - {}^2B_1$ energy differences. In both states the methyl groups prefer a conformation in which the in-plane C−H bonds eclipse the stronger of the two partial π bonds. This effect, but with *tert*-butyl rather than methyl groups, is responsible for the bond lengths found experimentally by Komatsu in **8a**.[11]

The predictions of the ground states of CPD radicals **9**−**33** should be amenable to experimental test. Measuring the size of the hyperfine coupling to the unique CPD ring hydrogen should make it possible to distinguish a $^2A_2$ ground state (hyperfine coupling constant small and positive) from a $^2B_1$ ground state (hyperfine coupling constant large and negative).[25] We hope that the results reported in this manuscript will stimulate experimental tests of our predictions.

Acknowledgment. We thank the National Science and Robert A. Welch Foundations for supporting this research. Some of the calculations reported here were performed on computers purchased with funds provided by the National Science Foundation under Grant CHE-0342824.

Supporting Information Available: Optimized geometries, energies, vibrational frequencies, and thermal corrections for **9a**−**33a** and for **9b**−**33b**, a version of Figure 7 giving the Hückel energies of the MOs, the calculated hyperfine coupling constant and spin density of the unique hydrogen in the $^2A_2$ and $^2B_1$ states for **9**−**33**, and the complete list of authors for ref 14. This material is available free of charge via the Internet at http://pubs.acs.org.

JA072314T

(24) The finding that tetrakis(ethano)COT prefers exocyclic over endocyclic localization by 2.3 kcal/mol[5] is *not* due to an electronic preference for the occupancy of orbital **b** in Fig 1 for X = CH_2. The symmetry of the HOMO of each ethano group is expected to favor donation into orbital **b**, leading to the occupation of orbital **a** and endocyclic localization. In fact, when the bond lengths in the eight-membered ring are constrained to be equal, we find that occupation of orbital **a** is, indeed, calculated to be favored. Therefore, the small preference for exocyclic double bonds, which is computed for tetrakis(ethano)COT at the geometries optimized for each type of localization, is almost certainly due to the longer bonds between the annelated carbons at the exocyclic geometry. The longer C−C bonds result in smaller amounts of strain within the four-membered rings.

(25) The calculated hyperfine coupling constants to the unique hydrogen in the $^2A_2$ and $^2B_1$ states of **9**−**33** are given in the Supporting Information.